applied sciences

MDPI

Article

Some Approaches for Light and Color on the Surface of Mars

Manuel Melgosa [1,*], Javier Hernández-Andrés [2], Manuel Sánchez-Marañón [3], Javier Cuadros [4] and Álvaro Vicente-Retortillo [5]

[1] Research Group FQM381 of the Andalusian Regional Government, Faculty of Sciences, University of Granada, 18071 Granada, Spain
[2] Department of Optics, Faculty of Sciences, University of Granada, 18071 Granada, Spain; javierha@ugr.es
[3] Department of Soil Science and Agricultural Chemistry, Faculty of Sciences, University of Granada, 18071 Granada, Spain; msm@ugr.es
[4] Natural History Museum, South Kensington, London SW7 5BD, UK; j.cuadros@nhm.ac.uk
[5] Astrobiology Center, National Research Council-National Institute of Aerospace Technology, 28850 Madrid, Spain; adevicente@cab.inta-csic.es
* Correspondence: mmelgosa@ugr.es; Tel.: +34-958-246364

Featured Application: To compute total spectral irradiance on the surface of Mars from a selected value of correlated color temperature in the range of 2333 K–5868 K.

Abstract: We analyzed the main colorimetric characteristics of lights on Mars' surface from 3139 total spectral irradiances provided by the COMIMART model (J. Space Weather Space Clim. 5, A33, 2015), modifying the parameters of 'solar zenith angle' and 'opacity', related to the time of day and the amount of dust in the atmosphere of Mars, respectively. Lights on Mars' surface have chromaticities that are mainly located below the Planckian locus, correlated color temperature in the range of 2333 K–5868 K, and CIE 2017 color fidelity indices above 93. For the 24 samples in the X-Rite ColorChecker® and an extreme dust opacity change from 0.1 to 8.1 in the atmosphere, the average color inconstancy generated by the change in Mars' light using the chromatic adaptation transform CIECAT16 was about 5 and 8 CIELAB units for solar zenith angles of 0° and 72°, respectively. We propose a method to compute total spectral irradiances on the surface of Mars from a selected value of correlated color temperature in the range of 2333 K–5868 K. This method is analogous to the one currently adopted by the International Commission on Illumination to compute daylight illuminants on the surface of Earth (CIE 015:2018, clause 4.1.2). The average accuracy of 3139 reconstructed total spectral irradiances using the proposed method was 0.9999558 using GFC (J. Opt. Soc. Am. A 14, 1007–1014, 1997) and 0.0009 $\Delta E_{u'v'}$ units, a value just below noticeable chromaticity differences perceptible by human observers at 50% probability. Total spectral irradiances proposed by Barnes for five correlated temperatures agreed with those obtained from the current proposed method: on the average, GFC = 0.9979521 and 0.0023 $\Delta E_{u'v'}$ units.

Keywords: colorimetry; sol-light; daylight; correlated color temperature; color inconstancy; Mars

Citation: Melgosa, M.; Hernández-Andrés, J.; Sánchez-Marañón, M.; Cuadros, J.; Vicente-Retortillo, Á. Some Approaches for Light and Color on the Surface of Mars. *Appl. Sci.* **2024**, *14*, 10812. https://doi.org/10.3390/app142310812

Academic Editor: Andrey Miroshnichenko

Received: 26 September 2024
Revised: 18 November 2024
Accepted: 20 November 2024
Published: 22 November 2024

1. Introduction

Both the Earth and Mars receive light from the Sun, but total (direct + diffuse) spectral irradiances on the surfaces of both planets are different for several reasons. For example, the average distances to the Sun from Earth and Mars are 0.98–1.02 and 1.38–1.67 AU (1 AU = 149.6 million km), respectively; temperatures (120–293 K) and atmospheric pressures (6–10 hPa) on Mars' surface are much lower than those on Earth; the thickness and chemical composition of the atmospheres of these two planets are very different, with the main gasses being N_2 (78%) on Earth and CO_2 (96%) on Mars. In particular, dust is ubiquitous in the Martian atmosphere, which plays a key role in climate.

Experimental measurements of the spectral power distribution of light on the surface of Earth (usually known as daylight) have been performed [1,2], and the results indicated

dependencies on geographical location, time of day, season, atmospheric conditions, etc. From measurements of spectral distributions of 622 samples of daylight performed at three different locations [1], the International Commission on Illumination (CIE) has proposed a model of daylight (see clause 4.1.2 in [3]). However, daylight remains an active research topic because it is most important for the right conditions for the development of life on Earth and many different applications. For example, the CIE Technical Committee 3–60 currently analyzes new daylight experimental measurements, the model for daylight proposed by the CIE has been revisited [4], and the CIE has proposed indoor and smoothed daylight illuminants for applications [3].

In contrast, our knowledge about light on Mars' surface is scarcer. Experimental measurements of light on the surface of Mars (sometimes designated as sol-light, because 'sols' is the name for Martian days) are much more difficult to obtain than those on the surface of Earth. Limitations in optical communications with very long distances [5], such as the available optical power at the transmitter, the size of optical apertures, and the sensitivity of the receiver, together with the limited number of filters in cameras installed on rovers, imply that current missions on Mars' surface provide irradiance data only at a few wavelengths in the visible and near-infrared range [6]. From a reduced set of 50 spectral irradiance samples provided by rovers on the Spirit and Opportunity missions, Barnes proposed five preliminary Mars illuminants with correlated color temperatures (CCTs) in the range of 4600 K–5400 K [7]. Barnes tried to collect a higher number of spectral irradiances on Mars' surface to develop definitive sol-light illuminants from a given CCT using the method employed by Judd et al. to obtain daylight illuminants [1], but, as far as we know, his goal was not completed.

When looking for the computation of true colors of objects on the surface of Mars, we must consider several questions. First, the CIE explicitly recommended that, in the interest of standardization, the D65 illuminant (a phase of daylight with a CCT of approximately 6500 K) be used whenever possible [3], but it seems that lights on the surface of Mars have CCTs that are considerably lower than 6500 K. Therefore, the assumption of D65 to compute colors on Mars surface is not realistic. Second, the CIE recommended performing color computations using spectral data in the range of 360–830 nm in steps of 1 nm [3], but on Mars, the total number of narrow spectral ranges sampled currently is only about 10–20, because of the reasons stated above. To solve this problem we can consider different approaches, like the use of inter- and extrapolation from measured spectral data [8], or the adoption of theoretical models providing spectral power distributions of light on Mars' surface [9]. In the current paper, we have used a widely accepted radiative transfer model named COMIMART [9], modifying the values of two of its parameters, 'solar zenith angle' and 'opacity', related to the time of sol (Martian day) and the amount of dust in Mars' atmosphere, respectively. The COMIMART model includes updated wavelength-dependent radiative properties of Martian dust [10–12] and other atmospheric constituents (gasses and water ice clouds), relies on the delta-Eddington approximation [13], and has been validated with the DISORT model [14].

After describing the materials and methods in Section 2, in Section 3.1, we analyze the colorimetric characteristics of lights provided by COMIMART, using some pairs of spectral irradiances on the surface of Mars to estimate the color inconstancy for the 24 samples in the Macbeth ColorChecker [15], currently known as the X-Rite ColorChecker®. In Section 3.2, we will use a high number of total spectral irradiances provided by COMIMART to propose a model generating spectral distributions of lights on the surface of Mars from a selected value of CCT (i.e., sol-light illuminants). This model is analogous to the one currently adopted by the CIE to compute daylight illuminants on Earth [3] and had good agreement with previous data [7]. We think that the use of advanced colorimetry and our proposal of a model for sol-light illuminants could help geologists perform accurate analyses of rocks, soils, and landscapes from Mars [16].

2. Materials and Methods

From the COMIMART model, we obtained 43 × 73 = 3139 total (direct + diffuse) spectral irradiances on the surface of Mars with a spectral range of 300–830 nm at steps of 5 nm (see Supplementary Material). Specifically, we considered 43 values for the 'opacity' (parameter named 'Tau', ranging from 0.1 to 8.5 in steps of 0.2) and 73 values for the 'solar zenith angle' (parameter named 'Angle', ranging from 0° to 72° in steps of 1°), assuming a latitude of 0°, a solar longitude of 0° (spring equinox in the Northern Hemisphere), and a surface albedo of 0.2. In the COMIMART model, the parameters of opacity and solar zenith angle are related to the amount of dust in the atmosphere and the time of day, respectively. For each of these 3139 spectral irradiances, we computed x,y chromaticity coordinates for the CIE 1931 colorimetric observer [3], values of CCT from a binary search method described in [17], distances from the Planckian locus (D_{uv}) [18], and values of the general color fidelity index (R_f) [19]. Positive/negative values of D_{uv} in the range of ±0.05 indicate 'white lights' with chromaticities above/below the Planckian locus. The index R_f improves the old CIE general color rendering index (R_a), representing how closely the color appearances of 99 samples are reproduced on average by a test light as compared to those under a reference illuminant with the same CCT. The higher the value of R_f (always in the range of 0–100), the closer the color appearance produced by the test source is to the reference source.

An object is said to be 'color inconstant' when its color appearance changes because of variations in the color and level of illumination [20]. This occurs with changes in the spectral irradiance of light on the surface of Mars (current the case), or when comparing objects on the surfaces of Mars and Earth. The definition of 'corresponding colors' is pairs of color stimuli that look alike when one is seen in one set of adaptation conditions and the other is seen in a different set [20]. Corresponding colors are computed using chromatic adaptation transforms (CATs), the core of color appearance models (CAMs) used in advanced colorimetry [21]. Here, we computed corresponding colors using the chromatic adaptation transform CIECAT16 embedded in CIECAM16 [22], assuming a constant adaptation luminance L_A of 63.7 cd/m^2, which is equivalent to an illuminance of 1000 lx, an average surround adaptation factor (F = 1), and with illuminant D65 and CIE 1964 colorimetric observer (X_n = 94.81, Y_n = 100.00, Z_n = 107.28) as reference conditions. From corresponding colors, we computed color inconstancy in CIELAB units, using as reference white illuminant D65 with CIE 1964 colorimetric observer. For homogeneous object colors, visual thresholds for human observers with normal color vision fall within the range of 0.55–1.10 CIELAB units [23].

The input of the CIE method to compute spectral power distributions of daylight illuminants is a value of CCT in the range of 4000 K–25,000 K [3]. The CIE method follows the next four steps: (1) Compute the x chromaticity coordinate using a third-degree polynomial equation of the inverse of CCT, which depends on the input CCT value being in the range of 4000 K–7000 K or 7000 K–25,000 K. This leads to values of x chromaticity coordinates in the range of 0.250–0.380. (2) Compute the y chromaticity coordinate using a two-degree polynomial equation from the value of the x chromaticity coordinate. (3) Compute coefficients M_1 and M_2 from values of x,y chromaticity coordinates. (4) Compute the spectral power distribution of the illuminant from M_1 and M_2 using tabulated values of three specific functions (average and two eigenvectors) obtained by principal component analysis [3]. In Section 3.2, we will propose a method for the computation of sol-light illuminants based on 3139 spectral total irradiances from the COMIMART model, analogous to the method proposed by the CIE for daylight illuminants [3], which was based on experimental measurements of spectral distributions of 622 samples of daylight compiled by Judd et al. [1].

For a given CCT, the accuracy of the reconstructed total spectral irradiance (sol-light illuminant) generated by our model, $E_R(\lambda_i)$, in comparison with the original one from COMIMART, $E(\lambda_i)$, has been assessed by the goodness of fit coefficient (GFC) defined in

Equation (1) [24]. GFC values are in the range of 0–1, because they represent the cosine of the angle between two vectors, with a value of 1 indicating a perfect fit.

$$\mathrm{GFC} = \frac{\left|\sum_{i=1}^{n} E(\lambda_i)\, E_R(\lambda_i)\right|}{\left|\sum_{i=1}^{n} E(\lambda_i)^2\right|^{1/2} \left|\sum_{i=1}^{n} E_R(\lambda_i)^2\right|^{1/2}} \quad (1)$$

The current CIE recommendation for the specification of chromaticity tolerances of light sources is the use of u′v′ circles [25]. Accordingly, in addition to the GFC, we also used Euclidean distances in the $u'v'$ diagram ($\Delta E_{u'v'}$ units) to assess the similitude between two given spectral irradiances. The size of a just-noticeable chromaticity difference at 50% probability is 0.0013 $\Delta E_{u'v'}$ units [25].

3. Results

3.1. Colorimetric Characteristics of Lights on Mars' Surface

As an example of the total (direct + diffuse) spectral irradiances from the COMIMART model, Figure 1 shows those obtained for solar zenith angles of 0°, 18°, 36°, 54°, and 72° for three opacity (Tau) values of 0.1, 4.1, and 8.1, corresponding to almost clear, dust storm, and extraordinarily strong dust storm conditions, respectively. As we can see, total spectral irradiances decrease when values of the solar zenith angle increase (in particular for angles above 18° approximately), and the maximum values of the curves are shifted towards higher wavelengths (more reddish lights) when opacity (Tau) increases.

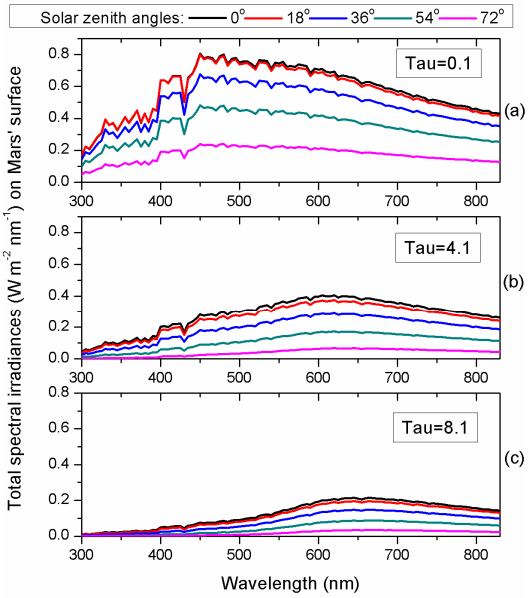

Figure 1. Examples of total (direct + diffuse) spectral irradiances on Mars' surface from the COMIMART model [9], considering three values of opacity (Tau) [0.1 (**a**), 4.1 (**b**), and 8.1 (**c**)] and five values of the solar zenith angle (0°, 18°, 36°, 54°, the 72°).

3.1.1. Correlated Color Temperature (CCT)

Figure 2 shows the histogram of CCTs we computed using the method indicated in [17] for 3139 total spectral irradiances provided by COMIMART. We found that CCTs of lights on Mars' surface are in the range of 2333 K–5868 K with an average value of 3984 K (standard deviation of 953 K), which is consistent with CCTs in the range of 4600 K–5400 K reported by Barnes [7]. Therefore, CCTs of lights on Mars' surface are lower and in a shorter range than lights on Earth's surface. Specifically, daylight illuminants proposed by CIE [3] have CCTs in the range of 4000 K–25,000 K, and two currently recommended CIE standard illuminants are D65 and D50, which have approximate CCTs of 6500 K and 5000 K, respectively. Accordingly, we can state that the currently recommended D65 illuminant

for use on Earth is not a realistic choice for work on Mars' surface. In Section 3.2 we will propose alternative sol-light illuminants which may be used in the future.

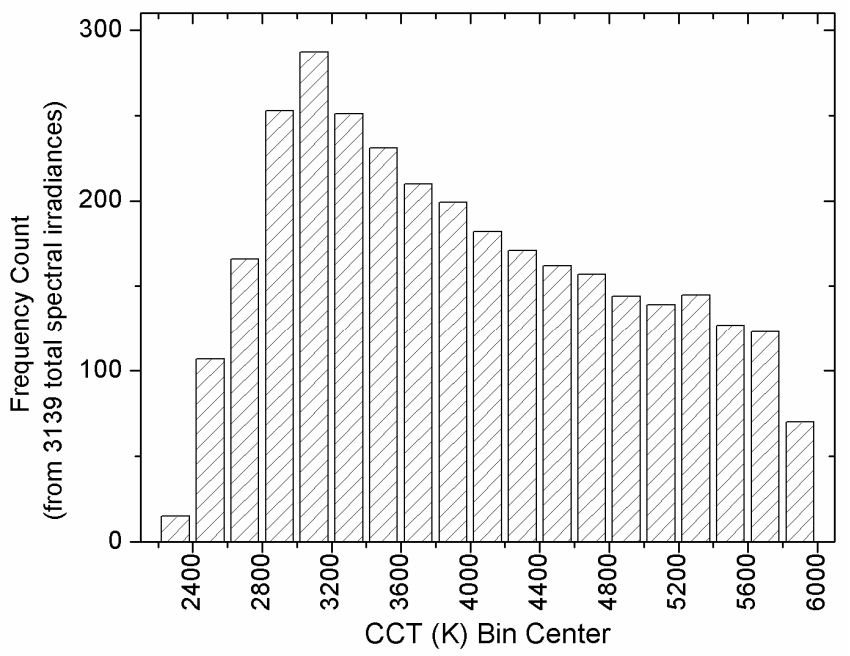

Figure 2. Histogram of correlated color temperatures (CCTs) corresponding to 3139 total spectral irradiances on Mars' surface provided by the COMIMART model [9].

Figure 3 illustrates changes in CCT for a few values of opacity (Tau) and solar zenith angles. As expected, we can see that the CCTs considerably decrease (more reddish lights) both when opacity (i.e., the amount of dust in the atmosphere) increases, and when the solar zenith angle increases from 0° to 72° (except for very low Tau values).

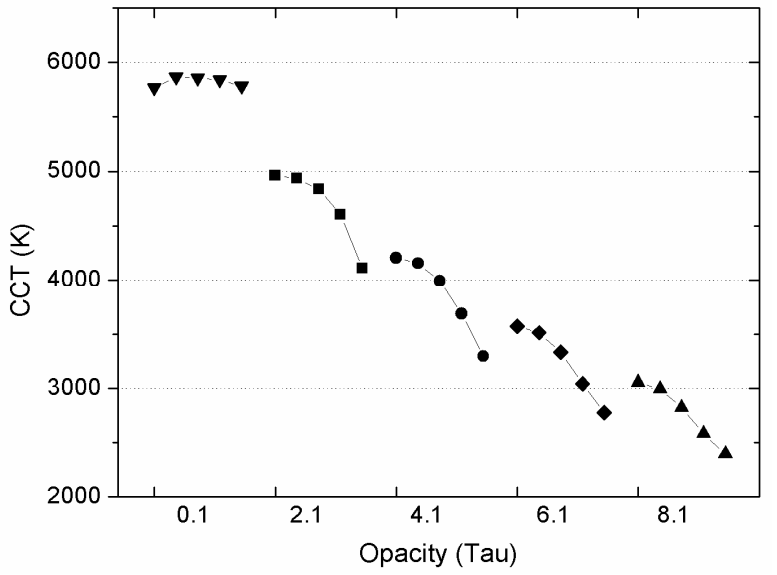

Figure 3. Correlated color temperatures (CCTs) for lights on Mars' surface with five values of opacity (Tau = 0.1, 2.1, 4.1, 6.1 and 8.1), and five values of zenith solar angle (0°, 18°, 36°, 54° and 72°, symbols in this order from left to right) for each opacity.

3.1.2. Distance from the Planckian Locus (D_{uv})

All 3139 lights on Mars' surface may be qualified as 'white lights' because their distances from the Planckian locus (D_{uv}) are lower than ±0.05 *uv* units [3,18]. More

specifically, Figure 4 shows that distances D_{uv} are slightly positive (i.e., points above the Planckian locus) only for very low opacity values (e.g., Tau = 0.1), and are increasingly negative when Tau values increase. Barnes already reported [7] that lights on Mars' surface had chromaticities below the Planckian locus, with the opposite happening for lights on Earth [1,3], which have chromaticities above the Planckian locus. Figure 4 also shows that as the solar zenith angle increases, the chromaticities of lights approach the Planckian locus (except for very low Tau values).

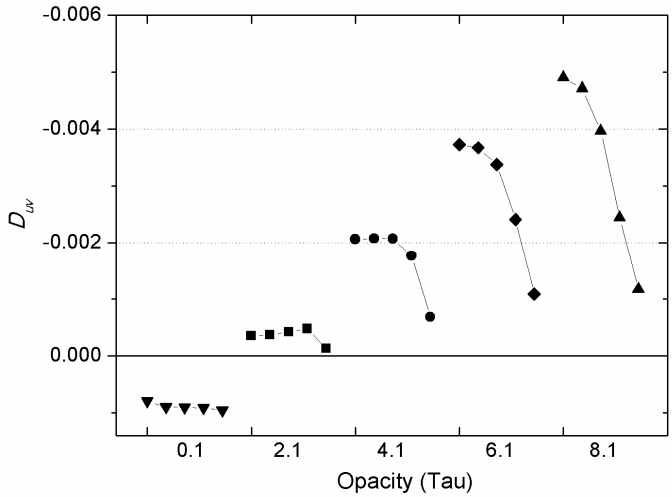

Figure 4. Distances from the Planckian locus (D_{uv}) [18] for lights on Mars' surface with five values of opacity (Tau = 0.1, 2.1, 4.1, 6.1, and 8.1) and five values of zenith solar angle (0°, 18°, 36°, 54°, and 72°, with symbols in this order from left to right) for each opacity.

3.1.3. CIE 2017 Color Fidelity Index (R_f)

Figure 5 indicates that lights on Mars' surface have high values on the CIE 2017 color fidelity index (R_f), which means that colors of objects illuminated by lights on the surface of Mars are similar enough to those under reference sources on Earth (daylights) with the same CCT [19]. Specifically, the ideal (maximum) value of R_f is 100 and, in our current case, the lowest value of R_f was 93.2 (Tau = 8.5 and solar zenith angle of 72°). Figure 5 shows that R_f generally decreases when opacity increases, while for high opacity values, R_f slightly decreases when the solar zenith angle increases.

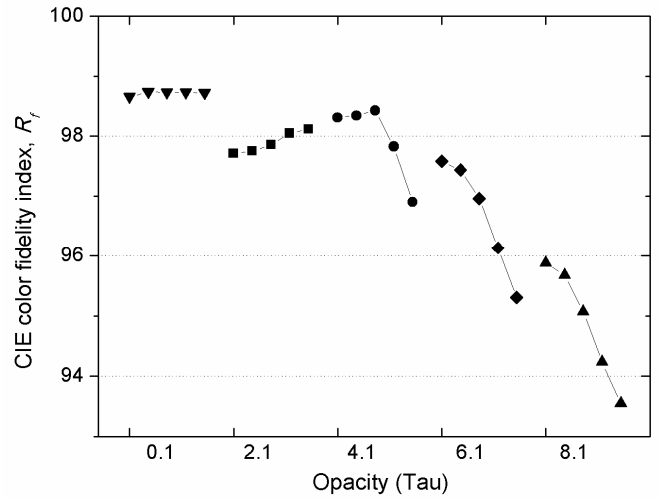

Figure 5. CIE 2017 color fidelity index (R_f) [19] for lights on Mars' surface with five values of opacity (Tau = 0.1, 2.1, 4.1, 6.1, and 8.1) and five values of zenith solar angle (0°, 18°, 36°, 54°, and 72°, with symbols in this order from left to right) for each opacity.

3.1.4. CIE *x*,*y* Chromaticity Coordinates

Figure 6 shows the *x*,*y* chromaticity coordinates of the 3139 total spectral irradiances obtained from the COMIMART model, corresponding to lights on Mars' surface, together with parts of the Planckian and daylight (light on Earth) loci. It can be noted that daylights defined by CIE only have CCTs higher than 4000 K [3], which implies that $x < 0.380$. As mentioned before, we can see that most lights on Mars' surface are located below the Planckian locus, while daylights on Earth's surface are located above, in agreement with previous results [7]. For any value of opacity (Tau), when the solar zenith angle increases, both chromaticity coordinates *x* and *y* increase (i.e., more reddish lights).

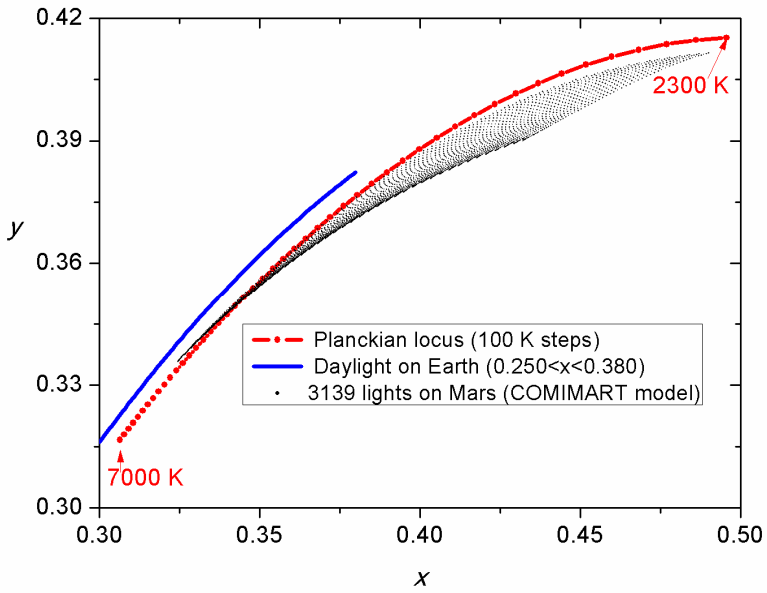

Figure 6. CIE *x*,*y* chromaticity coordinates for the 3139 lights on Mars' surface from the COMIMART model [9], in comparison with a part of the Planckian locus (red line) and Earth's daylight locus (blue line) established by CIE [3].

3.1.5. Color Inconstancy for Samples in the X-Rite ColorChecker®

We computed the corresponding colors [20] for the 24 samples in the X-Rite ColorChecker® [15], using the chromatic adaptation transform CIECAT16 [22] with reference condition illuminant D65 and CIE 1964 colorimetric observer for a constant adapting illuminance equivalent to 1000 lx. Next, we computed color inconstancy values [21] in CIELAB units for these samples under some pairs of lights on Mars' surface, as shown in Figures 7–9.

Figure 7 shows CIELAB color inconstancies for changes in the solar zenith angle from 0° to 72° considering five opacity (Tau) values. For the lowest opacity value (i.e., Tau = 0.1) the average color inconstancy in Figure 7 is 0.06 CIELAB units, and, in principle, none of the 24 samples should exhibit a perceptible color change when the solar zenith angle changes from 0° to 72° [23]. However, this change in solar zenith angle does generate average perceptible color changes, which increase with opacity, up to an average value of 3.4 CIELAB units (with a standard deviation of 2.3 CIELAB units) for Tau = 8.1. Similarly, Figure 8 shows CIELAB color inconstancies for changes in opacity from Tau = 0.1 for two values of the solar zenith angle (0° and 72°). From Figure 8, average color inconstancies increase in an approximately linear way with the change in opacity, and are highest for the solar zenith angle of 72° (Figure 8b). Only for a solar zenith angle of 0°, and when opacity changes from 0.1 to 2.1, do some of the samples in the X-Rite ColorChecker® appear not to exhibit perceptible color differences, because in this case, 15/24 samples (in particular all 6 achromatic samples in the ColorChecker®) exhibited color inconstancies below 1.0 CIELAB unit [23].

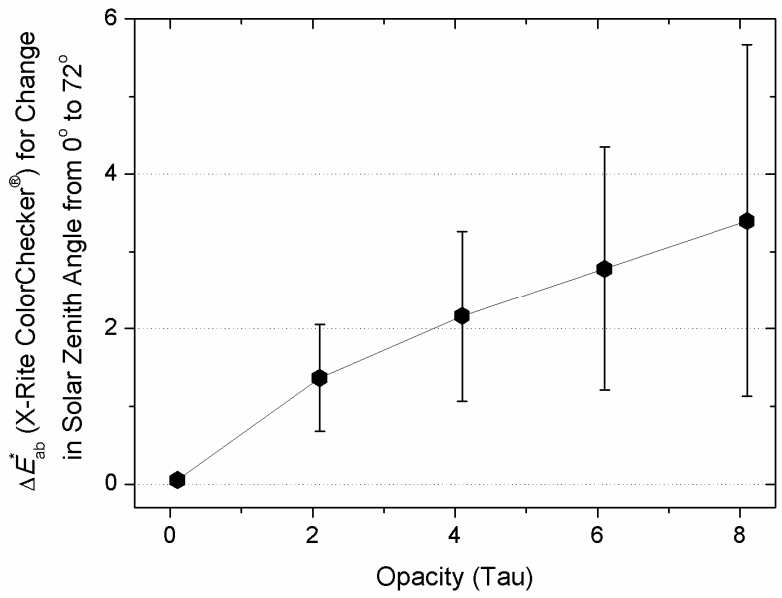

Figure 7. Average color inconstancies [21] and standard deviations (error bars) in CIELAB units for the 24 samples of the X-Rite ColorChecker® [15] and Mars' lights changing in solar zenith angle from 0° to 72° at five opacity values (Tau = 0.1, 2.1, 4.1, 6.1 and 8.1), using the chromatic adaptation transform CIECAT16 [22].

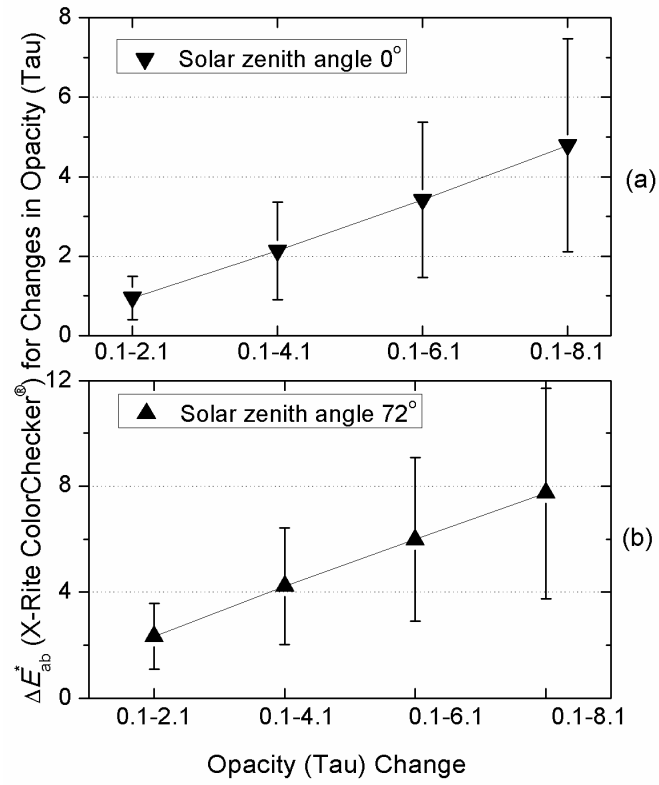

Figure 8. Average color inconstancies [21] and standard deviations (error bars) in CIELAB units for the 24 samples of the X-Rite ColorChecker® [15] and Mars' lights changing in opacity from Tau = 0.1 to increasing values of Tau up to 8.1, for two solar zenith angles, 0° (**a**) and 72° (**b**), using the chromatic adaptation transform CIECAT16 [22].

The color inconstancy is not the same for the 24 samples in the X-Rite ColorChecker® [15], numbered here in such a way that the last row of the chart includes the achromatic samples #19 (white) to #24 (black). As an example, Figure 9 shows the color shifts undergone by

each of the 24 samples when opacity has a very high change (from Tau = 0.1 to Tau = 8.1) and the solar zenith angle is 72°. Color shifts of six achromatic samples (#19–#24) are not well distinguished in Figure 9, but they are in the range from 1.8 (black sample #24) to 5.2 (white sample #19) CIELAB units, above the human visual threshold (0.55–1.10 CIELAB units [23]). An approximate visualization (Adobe Photoshop 22.1.0) of color shifts indicated in Figure 9 is provided by the two images of the X-Rite ColorChecker® shown in Figure 10.

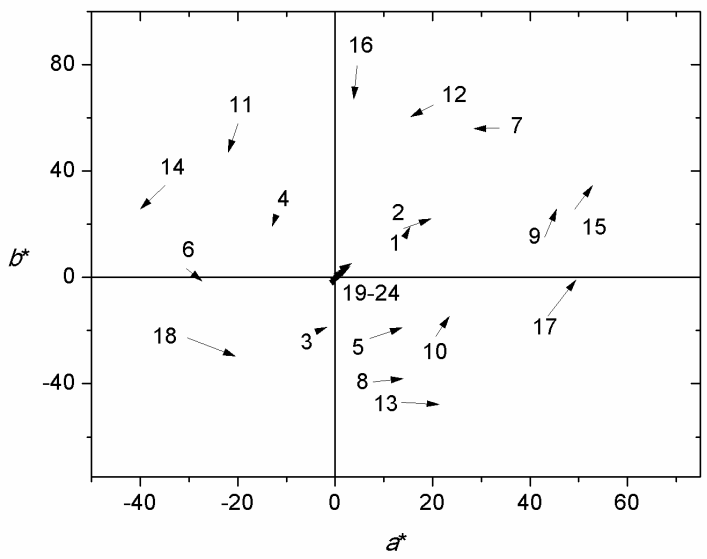

Figure 9. Color shifts in CIELAB *a* b** plane for the 24 samples in the X-Rite ColorChecker® (numbers in the arrows) [15], for a solar zenith angle of 72° and a change in opacity from Tau = 0.1 (origin of arrows) to Tau = 8.1 (end of arrows), using the chromatic adaptation transform CIECAT16 [22].

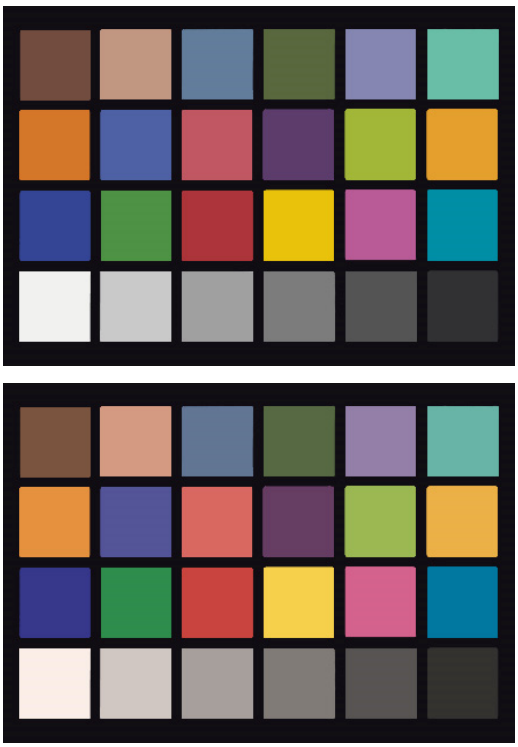

Figure 10. Approximate colors (Adobe Photoshop 22.1.0) of the 24 samples in the X-Rite ColorChecker® [15] for two light sources on Mars' surface with a solar zenith angle of 72° and opacity values (Tau) of 0.1 (**a**) and 8.1 (**b**).

3.2. Modeling Light on Mars' Surface from CCT

3.2.1. Proposal for a Model Analogous to the One Adopted by CIE for Daylight [3]

As indicated before, to model light on Mars' surface, we followed the method proposed by Judd et al. [1] and adopted by CIE (clause 4.1.2 in [3]), which was developed from 622 experimental measurements of spectral power distributions on Earth's surface and used CCT as the only input parameter. The main difference in our current model is that it starts from 3139 theoretical spectral irradiances obtained from the COMIMART model (see Section 3.1) rather than from experimental measurements.

First, we normalized the 3139 total spectral irradiances to the irradiance at 560 nm. Second, using the method introduced in [17] we computed their CCTs and x,y chromaticity coordinates. Next, the values of the x coordinate were fitted to a third-order polynomial of the inverse of CCT with a high accuracy (R^2 = 0.9994), obtaining Equation (2). Depending on the CCT value, the method proposed by CIE [1,3] used two different equations with the same format as Equation (2). However, for lights on Mars' surface, the range in CCT is shorter than that for lights on Earth, and Equation (2) is sufficient to obtain the x coordinate values from CCT. Equation (3) shows a parabolic function fitting values of the y coordinate from values of the x coordinate for the 3139 total spectral irradiances (R^2 = 0.9907). Next, Equations (4) and (5) provide values of coefficients M_1 and M_2 from x,y chromaticity coordinates. Finally, Equation (6) provides the spectral power distribution of light on Mars' surface $S_M(\lambda)$ from the mean $S_0(\lambda)$ and two first eigenvectors, $V_1(\lambda)$ and $V_2(\lambda)$, computed by principal component analysis. From these two first eigenvectors, we can explain 99.96% of the information in the original 3139 total spectral irradiance data. Table A1 provides values of functions $S_0(\lambda)$, $V_1(\lambda)$, and $V_2(\lambda)$ from 300 nm to 830 nm in steps of 5 nm. Figure 11 shows the functions $S_0(\lambda)$, $V_1(\lambda)$, and $V_2(\lambda)$, with each one normalized to its corresponding norm. Previously mentioned Equations (2)–(6) constitute our proposal for modeling lights on Mars' surface (sol-light illuminants) for a selected CCT in the range of 2333 K–5868 K (see the Excel file in the Supplementary Materials), and are as follows:

$$x = \frac{7.1528 \times 10^8}{T_{cp}^3} - \frac{8.3336 \times 10^5}{T_{cp}^2} + \frac{0.9416 \times 10^3}{T_{cp}} + 0.1845 \quad (2)$$

$$y = -1.6343\, x^2 + 1.7752\, x - 0.0669 \quad (3)$$

$$M_1 = \frac{-9.0797 + 59.0649\, x - 36.9329\, y}{-0.3418 - 1.3063\, x + 4.7227\, y} \quad (4)$$

$$M_2 = \frac{13.5231 + 35.7428\, x - 73.4435\, y}{-0.3418 - 1.3063\, x + 4.7227\, y} \quad (5)$$

$$S_M(\lambda) = S_0(\lambda) + M_1 V_1(\lambda) + M_2 V_2(\lambda) \quad (6)$$

Table 1 shows basic statistics on the accuracy of the sol-light proposed model (Equations (2)–(6)) for the 3139 total spectral irradiances generated from COMIMART. Specifically, we compared each total spectral irradiance generated by COMIMART with the total spectral irradiance computed from our model (CCT computed by the method in [17]), using GFC (Equation (1)) [24] and $\Delta E_{u'v'}$ units [25]. Figure 12 shows the total spectral irradiances for the median (0.9999839) and worst (0.9996321) GFC values. As we can see, the accuracy of our proposed model to compute sol-light illuminants is very high. The average distance between original and reconstructed total spectral irradiances is 0.00090 $\Delta E_{u'v'}$ units, which is below the value of a just-noticeable chromaticity difference at 50% probability (0.0013 $\Delta E_{u'v'}$ units [25]). The maximum distance in Table 1 (0.00336 $\Delta E_{u'v'}$ units) is about three Standard Deviations of Color Matching (3-SDCM = 0.0033 $\Delta E_{u'v'}$ units [25]), which is usually considered as the acceptable chromaticity tolerance for light sources and observers with normal color vision.

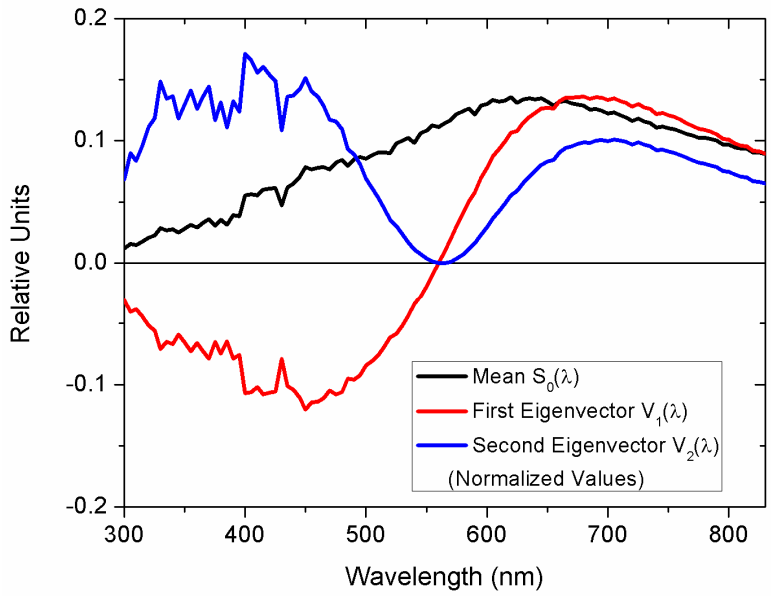

Figure 11. Functions $S_0(\lambda)$, $V_1(\lambda)$, and $V_2(\lambda)$ in Equation (6) and Table A1, normalized to their corresponding norms, computed using principal component analysis from 3139 normalized total (direct + diffuse) spectral irradiances on Mars' surface.

Table 1. Comparison between 3139 total spectral irradiances generated by COMIMART [9] and obtained by our sol-light model (Equations (2)–(6)) using CCTs computed from [17].

Basic Statistics Parameters	GFC (Equation (1))	$\Delta E_{u'v'}$ Units [25]
Average	0.9999558	0.00090
Standard Deviation	0.0000630	0.00079
Best fit	0.9999998	0.00001
Worst fit	0.9996321	0.00336

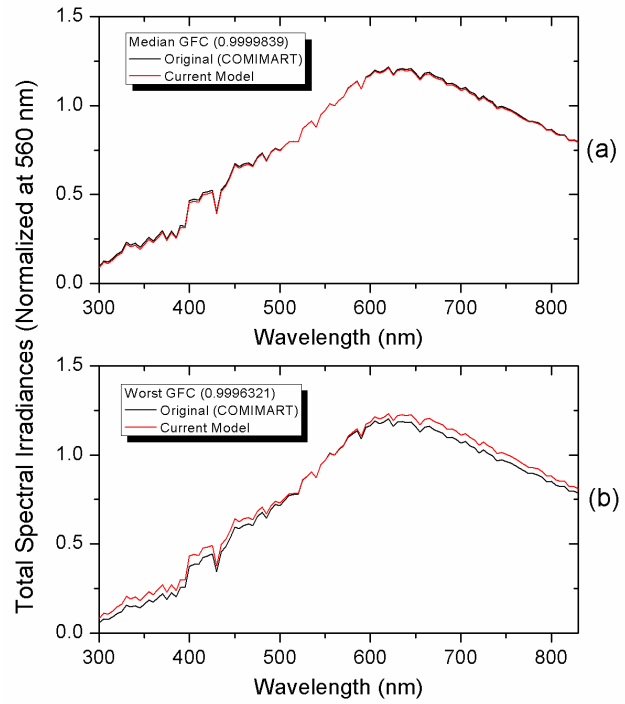

Figure 12. Median (**a**) and worst (**b**) predictions of 3139 total spectral irradiances from COMIMART using our model (Equations (2)–(6)), with CCTs computed from [17].

3.2.2. Comparison with Spectral Irradiances Reported by Barnes [7]

As indicated before, current cameras in rovers working on Mars' surface only provide measurements of spectral irradiances at a few wavelengths within the visible range, which prevents accurate computations of tristimulus values (the first quantitative specification of color) for any object on Mars' surface. From some measurements provided by rovers, Barnes [7] compiled a set of 50 spectral irradiances (not given in his paper) and used them to propose five specific Mars illuminants, named M46, M48, M50, M52, and M54 (the last two numbers in these designations indicate the CCTs in Kelvin of these illuminants divided by 100). From Figure 4 in reference [7], we used WebPlotDigitizer v4.2 [26] to obtain numerical values of five Mars illuminants proposed by Barnes, and computed their corresponding CCTs using the method indicated in [17]. From these five CCTs, we computed sol-light illuminants using our model in Section 3.2.1. The illuminants proposed by Barnes and those obtained from our model are shown in Figure 13a. Specifically, Table 2 shows information about the similitude between the five pairs of spectra shown in Figure 13a (i.e., between spectral irradiances at each temperature for Barnes' and our current model). Figure 13b shows that small differences between total spectral irradiances from the model in Section 3.2.1 and Barnes illuminants are similar for the five CCTs and are mainly located in the region below 450 nm, approximately.

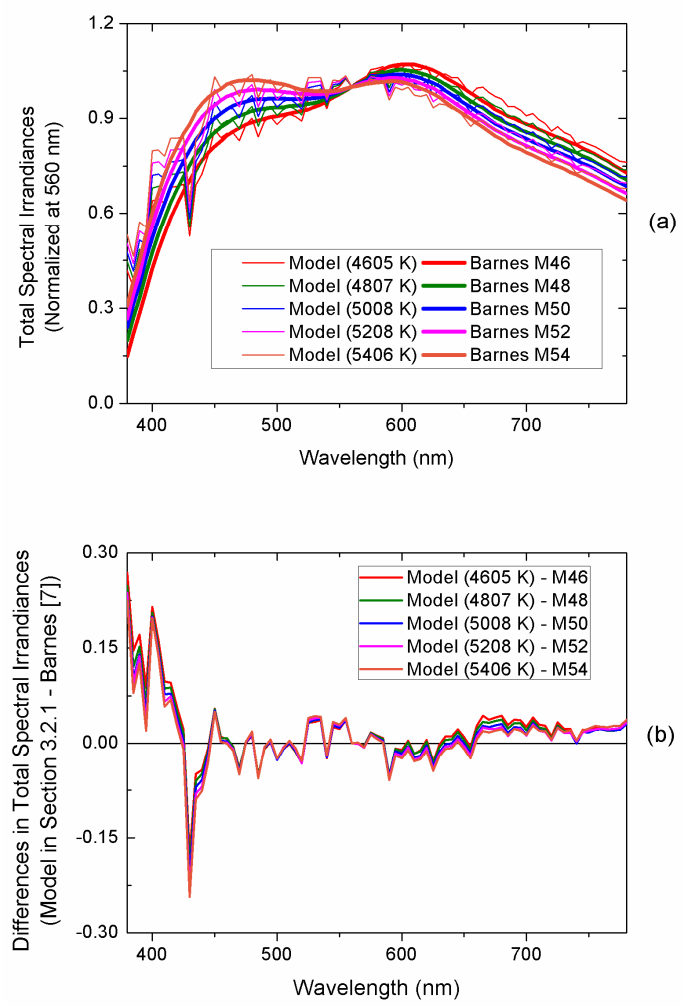

Figure 13. Total spectral irradiances on Mars' surface from the model in Section 3.2.1 with indicated CCTs (thin lines) and those proposed by Barnes [7] (thick lines) (**a**). Differences between total spectral irradiances from the model in Section 3.2.1 and from those proposed by Barnes (subtraction: *our model–Barnes' model*) (**b**).

Table 2. Comparison between spectral irradiancies of five illuminants (M46, M48, M50, M52, and M54) proposed by Barnes [7] and those obtained by our sol-light model (Equations (2)–(6)) with CCTs computed from [17].

Basic Statistics Parameters	GFC (Equation (1))	$\Delta E_{u'v'}$ Units [25]
Average	0.9979521	0.00227
Standard Deviation	0.0001299	0.00077
Best fit	0.9980494	0.00130
Worst fit	0.9977288	0.00322

4. Discussion

Color science teaches [3] that, in a first approach, the perceived color of an object depends on three main factors: the spectral power distribution of the light source illuminating the object, the spectral reflectance/transmittance of the object, and the spectral sensitivities of photoreceptors in our retina. In the next paragraphs, we add some considerations about each one of these three factors in our current case.

Given the interest of applied physics for the better understanding of Mars [6,27–29], the current paper focused on lights on Mars' surface, considering their colorimetric characteristics (Sections 3.1.2–3.1.4), and proposed a model to compute Mars (sol-light) illuminants from an input CCT in the range of 2333 K–5868 K (Section 3.2.1). This model is analogous to the one recommended by CIE for daylight illuminants on Earth (clause 4.1.2 in [3]), but is based on 3139 theoretical spectral irradiances from the COMIMART model. Our model produced a very good match with the results generated by Barnes [7] using a limited number of 50 experimental irradiances from vehicles on Mars (Section 3.2.2). The spectra generated by our model display noise (mainly dips) that is present in the standard solar spectrum AM0 [30], while spectra published by Barnes appear as smooth curves (Figure 13). However, the similarity of results is encouraging. As expected, results in Table 2 show greater differences than those in Table 1, given that the model proposed in Section 3.2.1 was based on 3139 total spectral irradiances, not on the five illuminants proposed by Barnes. However, even in the case where the comparison between our model and Barnes' results is poorest (M54; Figure 13), we found a high value of GFC (0.9977288) and a distance of 0.00322 $\Delta E_{u'v'}$ units, which is lower than three Standard Deviations of Color Matching (3-SDCM), the usual acceptable chromaticity tolerance for light sources and observers with normal color vision [25]. This good match justifies further progress with our model.

While D65 and D50 are the two currently CIE-recommended standard daylight illuminants [3], in the case of Mars, it seems appropriate to choose some sol-light illuminants with a lower CCT. For example, the average CCT corresponding to our 3139 total spectral irradiances is 3984 K (approximately, an M40 illuminant). This relatively low CCT value is attributable to the fact that we included high opacity values in our model. The average illuminant from Barnes has a CCT of around 5000 K (M50).

Regarding objects analyzed in the current paper, we selected the 24 samples in the X-Rite ColorChecker® [15] because they are considered to be a small representative set of familiar objects found on Earth's surface. Obviously, rock and soil samples that are analogous to those on Mars observed from orbit [31] or in situ [32–34] are much more interesting and will be considered in future work.

In relation to the sensitivity of the photoreceptors in the human retina, here, we followed current CIE recommendations [3] and adopted the CIE 1931 colorimetric observer for computations of CCT. However, the CIE 1964 colorimetric color observer was preferred to compute corresponding colors and color inconstancies of X-Rite ColorChecker® samples, because we assumed that most objects in our everyday life subtend viewing angles greater than 4°. Currently, the CIE 1964 colorimetric color observer is assumed in most practical and industrial color applications, excluding the analysis of complex images. In the current paper, we used several tools of advanced colorimetry [20,21], such as the computation of corresponding colors and color inconstancy indices. Such tools are necessary when comparing the colors of objects under different light sources, as emphasized in [16], whose

reference included results from a specific visual experiment (our current paper does not include any visual experiment). Here, we have assumed the last chromatic adaptation transform adopted by CIE, CIECAT16 [22], although considerable future basic research about CATs can be expected given the influence of the illuminance level, degree of adaptation, surrounding field, three-dimensional objects, etc.

5. Conclusions

From 3319 total (direct + diffuse) spectral irradiances provided by the radiative transfer model COMIMART [9], we analyzed some main colorimetric characteristics of lights on Mars' surface and color inconstancies for the 24 samples in the X-Rite ColorChecker® [15]. In addition, from the mentioned total spectral irradiances, we have proposed a model to compute Mars (sol-light) illuminants from a specific CCT value in the range of 2333 K–5868 K. This model is analogous to the one currently proposed by CIE to compute daylight illuminants on Earth (clause 4.1.2 in [3]). Results provided by the proposed model reasonably agreed with those previously reported by Barnes [7]. The current main CIE illuminant for Earth (i.e., the D65 illuminant) is not appropriate for use on Mars because its CCT is outside the range of lights on Mars' surface.

Supplementary Materials: The following supporting information can be downloaded at: https://www.mdpi.com/article/10.3390/app142310812/s1. The .zip file "Spectral curves" in the Supplementary Materials contains the spectral irradiances generated with the radiative transfer model COMIMART for the 3139 scenarios defined by the atmospheric opacity (tau) and the solar zenith angle. Each of the 43 .txt files in the .zip file contain the spectral irradiances for the opacity specified in the name of the file; in each file, columns 2−74 contain the spectral irradiances for the solar zenith angles defined in the first row (from 0° to 72°) as a function of wavelength, indicated in the first column; the line immediately above the data contains additional information of the other model inputs. The Excel file "Sol-light model" in the Supplementary Materials uses any input CCT in the range of 2300–5900 K (cell B1), providing the total spectral irradiance (sol-light illuminant) in column H from the model proposed in Section 3.2.1.

Author Contributions: Conceptualization, M.M., J.H.-A., M.S.-M. and Á.V.-R.; methodology, M.M. and J.H.-A.; software, J.H.-A. and Á.V.-R.; validation, M.M., M.S.-M. and J.C.; formal analysis, M.M. and J.H.-A.; investigation, M.M., J.H.-A., M.S.-M., J.C. and Á.V.-R.; resources, Á.V.-R.; data curation, Á.V.-R. and J.H.-A.; writing—original draft preparation, M.M.; writing—review and editing, J.H.-A., Á.V.-R., M.S-M. and J.C.; supervision, J.C. and Á.V.-R.; project administration, M.M.; funding acquisition, M.M. All authors have read and agreed to the published version of the manuscript.

Funding: This research was funded by MICIU/AEI/10.13039/501100011033 and ERDF/EU, grants PID2022-138031NB-I00 and PID2021-126719OB-C41.

Data Availability Statement: The data presented in this study are available in the article and Supplementary Materials.

Acknowledgments: Francisco González-Galindo, Department of Solar System, Institute of Astrophysics of Andalucía (National Research Council), Granada, Spain. María Dolores Molina Fernández, Scientific Photography Unit, Center for Scientific Instrumentation, University of Granada, Spain.

Conflicts of Interest: The authors declare no conflicts of interest.

Appendix A

Table A1 shows values of functions $S_0(\lambda)$, $V_1(\lambda)$, and $V_2(\lambda)$, introduced in Equation (6), which are used in our model to compute total spectral irradiances on Mars' surface (sol-light illuminants) for a CCT in the range of 2333 K–5868 K (see Section 3.2.1).

Table A1. Functions $S_0(\lambda)$, $V_1(\lambda)$, and $V_2(\lambda)$ introduced in Equation (6) from 300 nm to 830 nm in steps of 5 nm.

Wavelength (nm)	$S_0(\lambda)$	$V_1(\lambda)$	$V_2(\lambda)$
300	0.10725233	−0.03076008	0.06844971
305	0.14314817	−0.04081334	0.09011341
310	0.13480432	−0.03818179	0.08359607
315	0.1573771	−0.04424705	0.09598776
320	0.18561136	−0.05175401	0.11114268
325	0.20224757	−0.05587057	0.11865292
330	0.25916588	−0.07085768	0.14865228
335	0.23980736	−0.06482405	0.13420139
340	0.25041275	−0.06685835	0.13644633
345	0.22359765	−0.05890594	0.11838833
350	0.25298031	−0.06569689	0.1298993
355	0.2846522	−0.07279801	0.14147285
360	0.26233759	−0.06600863	0.1259613
365	0.29330715	−0.07254302	0.13580607
370	0.32472845	−0.07887415	0.14473207
375	0.27316413	−0.06510301	0.11699688
380	0.32013008	−0.07480053	0.13154592
385	0.28168677	−0.06447666	0.11088027
390	0.35154298	−0.07876859	0.13237012
395	0.3446681	−0.07554804	0.12398884
400	0.49978178	−0.10710084	0.17157268
405	0.50632297	−0.10602631	0.16572196
410	0.49904148	−0.10207684	0.15562103
415	0.54089798	−0.1080432	0.16063205
420	0.54621077	−0.10653344	0.15445321
425	0.55407447	−0.10552727	0.14921303
430	0.42303878	−0.07869746	0.10856006
435	0.55664006	−0.10119272	0.13625538
440	0.58709675	−0.1043753	0.13728601
445	0.63639233	−0.11073059	0.14238576
450	0.70705757	−0.12039565	0.15134
455	0.6877586	−0.11445161	0.14046251
460	0.70225927	−0.11389605	0.13611401
465	0.70631366	−0.11118103	0.12887778
470	0.69003141	−0.10493713	0.11747993
475	0.73774396	−0.10786912	0.1161126
480	0.75910986	−0.1061701	0.10937022
485	0.71499013	−0.09513017	0.09332047
490	0.76185075	−0.09585772	0.08907384
495	0.78155613	−0.09239224	0.08086307
500	0.7676049	−0.0846485	0.06934917
505	0.79265998	−0.08088801	0.06161015
510	0.81194358	−0.07595842	0.05336985
515	0.81289874	−0.06894467	0.04428013
520	0.8081881	−0.0613061	0.03560266
525	0.881142	−0.05877756	0.03046008
530	0.90037581	−0.05167395	0.0235066
535	0.91945737	−0.044082	0.01723362
540	0.88400714	−0.03394228	0.01108406
545	0.95360928	−0.02745046	0.00719103
550	0.97415929	−0.01865847	0.00368306
555	1.01139987	−0.00965108	0.00128458
560	1	0	0

Table A1. *Cont.*

Wavelength (nm)	$S_0(\lambda)$	$V_1(\lambda)$	$V_2(\lambda)$
565	1.02775098	0.00968364	-6.33×10^{-5}
570	1.04890403	0.01958173	0.00107897
575	1.09682211	0.03035998	0.00349657
580	1.11552803	0.04059586	0.00703414
585	1.13584869	0.05081217	0.01163544
590	1.0928715	0.05752547	0.01621408
595	1.15921636	0.06957667	0.02305681
600	1.1709624	0.07822551	0.02949436
605	1.19875526	0.08742301	0.03657909
610	1.18672394	0.09306639	0.04240896
615	1.19683764	0.09975484	0.04880209
620	1.21796488	0.10690224	0.05552769
625	1.17770753	0.10806878	0.05908548
630	1.20526742	0.11497969	0.06572705
635	1.21129693	0.11961103	0.07111549
640	1.20518108	0.12271871	0.0755468
645	1.211332	0.12675747	0.0804719
650	1.18695464	0.12724743	0.08300751
655	1.15750621	0.12677035	0.08469759
660	1.18610163	0.13236706	0.0903112
665	1.19278661	0.13532168	0.09403341
670	1.17645699	0.1353944	0.0955923
675	1.16540585	0.13579348	0.09719937
680	1.15822675	0.13639793	0.09878767
685	1.13093451	0.13439206	0.09831388
690	1.13370116	0.13574917	0.10014826
695	1.1219074	0.13519072	0.10044241
700	1.1002169	0.13327072	0.09959695
705	1.10941517	0.13495554	0.10134151
710	1.08686373	0.13265233	0.09999346
715	1.07334256	0.13132455	0.09927908
720	1.04532117	0.12810639	0.09704034
725	1.06180378	0.13024012	0.09877115
730	1.04025061	0.12761567	0.09681577
735	1.02944708	0.12622384	0.09572203
740	0.99679033	0.12207816	0.09247554
745	1.00480394	0.12284497	0.09289088
750	0.99376811	0.12121823	0.09144012
755	0.98330058	0.11947781	0.0901013
760	0.96841099	0.11715993	0.0882852
765	0.95266277	0.11470901	0.08633446
770	0.93686498	0.11223166	0.08433648
775	0.922595	0.1099238	0.08244486
780	0.9195483	0.10893849	0.08152787
785	0.91182118	0.10738633	0.08017343
790	0.89869736	0.10519966	0.07833933
795	0.87178158	0.10141983	0.07532222
800	0.87298935	0.1009289	0.07475232
805	0.85278797	0.09797984	0.07236832
810	0.84262005	0.09620919	0.07086448
815	0.84240739	0.09558593	0.07021073
820	0.8133602	0.09171438	0.06718019
825	0.81399557	0.09121213	0.06662654
830	0.80292511	0.0894072	0.06512605

References

1. Judd, D.B.; MacAdam, D.L.; Wyszecki, G. Spectral distribution of typical daylight as a function of correlated color temperature. *J. Opt. Soc. Am.* **1964**, *54*, 1031–1040. [CrossRef]
2. Hernández-Andrés, J.; Romero, J.; Nieves, J.L. Color and spectral analysis of daylight in southern Europe. *J. Opt. Soc. Am.* **2001**, *18*, 1325–1335. [CrossRef] [PubMed]
3. International Commission on Illumination. *CIE 015:2018. Colorimetry*, 4th ed.; CIE Central Bureau: Vienna, Austria, 2018; ISBN 978-3-902842-13-8. [CrossRef]
4. Diakite-Kortlever, A.; Weber, N.; Knoop, M. Reconstruction of daylight spectral power distribution based on correlated color temperature: A comparative study between the CIE approach and localized procedures in assessing non-image forming effects. *Leukos* **2023**, *19*, 118–145. [CrossRef]
5. Andrekson, P. Optical communication in very long space links. In Proceedings of the Book of Abstracts VI International Conference on Application of Optics and Photonics, AOP2024, Aveiro, Portugal, 16–19 July 2024; ISBN 978-989-8798-09-1.
6. Bell III, J.F.; Godber, A.; McNair, S.; Caplinger, M.A.; Maki, J.N.; Lemmon, M.T.; Van Beek, J.; Malin, M.C.; Wellington, D.; Kinch, K.M.; et al. The Mars Science Laboratory Curiosity rover Mastcam instruments: Preflight and in-flight calibration, validation, and data archiving. *Earth Space Sci.* **2017**, *4*, 396–452. [CrossRef]
7. Barnes, D. Mars Rover Colour Vision: Generating the True Colours of Mars. The 12th Symposium on Advanced Space Technologies in Automation and Robotics. 2013. Available online: http://robotics.estec.esa.int/ASTRA/Astra2013/Papers/barnes_2811165.pdf (accessed on 18 November 2024).
8. Wang, A.; Zhao, B.; Li, J.; Luo, M.R.; Pointer, M.R.; Melgosa, M.; Li, C. Interpolation, extrapolation, and truncation in computations of CIE tristimulus values. *Color Res. Appl.* **2017**, *42*, 10–18. [CrossRef]
9. Vicente-Retortillo, A.; Valero, F.; Vázquez, L.; Martínez, G.M. A model to calculate solar radiation fluxes on the Martian surface. *J. Space Weather Clim.* **2015**, *5*, A33. [CrossRef]
10. Wolff, M.J.; Smith, M.D.; Clancy, R.T.; Arvidson, R.; Kahre, M.; Seelos IV, F.; Murchie, S.; Savijärvi, H. Wavelength dependence of dust aerosol single scattering albedo as observed by the Compact Reconnaissance Imaging Spectrometer. *J. Geophys. Res-Planet* **2009**, *114*, E00D04. [CrossRef]
11. Wolff, M.J.; Clancy, R.T.; Goguen, J.D.; Malin, M.C.; Cantor, B.A. Ultraviolet dust aerosol properties as observed by MARCI. *Icarus* **2010**, *208*, 143–155. [CrossRef]
12. Connour, K.; Wolff, M.J.; Schneider, N.M.; Deighan, J.; Lefèvre, F.; Jain, S.K. Another one derives the dust: Ultraviolet dust aerosol properties retrieved from MAVEN/IUVS data. *Icarus* **2022**, *387*, 115177. [CrossRef]
13. Joseph, J.H.; Wiscombe, W.J.; Weinman, J.A. The delta-Eddington approximation for radiative flux transfer. *J. Atmos. Sci.* **1976**, *33*, 2452–2459. [CrossRef]
14. Stamnes, K.; Tsay, S.-C.; Wiscombe, W.; Jayaweera, K. Numerically stable algorithm for discrete-ordinate-method radiative transfer in multiple scattering and emitting layered media. *Appl. Optics* **1988**, *27*, 2502–2509. [CrossRef]
15. McCamy, C.S.; Marcus, H.; Davidson, J.G. A color-rendition chart. *J. Appl. Photogr. Eng.* **1976**, *2*, 95–99.
16. Robert, E.; Shen, C.; Estribeau, M.; Cucchetti, E.; Fairchild, M. Color correction of Mars images: A study of illumination discrimination along solight locus. *J. Imaging Sci. Technol.* **2023**, *67*, 050410. [CrossRef]
17. Hernández-Andrés, J.; Lee, R.L.; Romero, J. Calculating correlated color temperatures across the entire gamut of daylight and skylight chromaticities. *Appl. Optics* **1999**, *38*, 5703–5709. [CrossRef]
18. Ohno, Y. Practical use and calculation of CCT and Duv. *Leukos* **2014**, *10*, 47–55. [CrossRef]
19. International Commission on Illumination. *CIE 224:2017. CIE 2017 Colour Fidelity Index for Accurate Scientific Use*; CIE Central Bureau: Vienna, Austria, 2017; ISBN 978-3-902842-61-9.
20. Berns, R.S. *Billmeyer and Saltzman's Principles of Color Technology*, 3rd ed.; John Wiley & Sons, Inc.: Hoboken, NJ, USA, 2000; Appendix F; ISBN 0-471-19459-X.
21. Fairchild, M.D. *Color Appearance Models*, 2nd ed.; Chapters 8 and 9; John Wiley & Sons. Ltd.: Hoboken, NJ, USA, 2005; ISBN 0-470-01216-1.
22. International Commission on Illumination. *CIE 248:2022. The CIE 2016 Colour Appearance Model for Colour Management Systems: CIECAM16*; CIE Central Bureau: Vienna, Austria, 2022; Annex A; ISBN 978-3-902842-94-7.
23. Huang, M.; Cui, G.; Melgosa, M.; Sánchez-Marañón, M.; Li, C.; Luo, M.R.; Liu, H. Power functions improving the performance of color-difference formulas. *Opt. Express* **2015**, *23*, 597–610. [CrossRef]
24. Romero, J.; García-Beltrán, A.; Hernández-Andrés, J. Linear bases for representation of natural and artificial illuminants. *J. Opt. Soc. Am. A* **1997**, *14*, 1007–1014. [CrossRef]
25. International Commission on Illumination. *CIE TN 001:2014. Chromaticity Difference Specification for Light Sources*; CIE Central Bureau: Vienna, Austria, 2014. Available online: https://cie.co.at/publications/chromaticity-difference-specification-light-sources (accessed on 18 November 2024).
26. Roatgi, A. WebPlotDigitizer. Available online: https://apps.automeris.io/wpd4/ (accessed on 18 November 2024).
27. Murcia-Piñeros, J.; Prado, A.F.B.A.; Dimino, I.; de Moraes, R.V. Optimal gliding trajectories for descent on Mars. *Appl. Sci.* **2024**, *14*, 7786. [CrossRef]
28. Zhang, T.; Peng, S.; Jia, Y.; Tian, H.; Sun, J.; Yan, C. Slip estimation for Mars rover Zhurong based on data drive. *Appl. Sci.* **2022**, *12*, 1676. [CrossRef]

29. Rodin, A.; Vinogradov, A.; Zenevich, S.; Spiridonov, M.; Gazizov, I.; Kazakov, V.; Meshcherinov, V.; Golovin, I.; Kozlova, T.; Lebedev, Y.; et al. Martian multichannel diode laser spectrometer (M-DLS) for in-situ atmospheric composition measurements on Mars onboard ExoMars-2022 landing platform. *Appl. Sci.* **2020**, *10*, 8805. [CrossRef]
30. National Renewable Energy Laboratory (NREL). 2000 ASTM Standard Extraterrestrial Spectrum Reference E-490-00. Available online: https://www.nrel.gov/grid/solar-resource/spectra-astm-e490.html (accessed on 18 November 2024).
31. Bell III, J.F.; Wolff, M.J.; Malin, M.C.; Calvin, W.M.; Cantor, B.A.; Caplinger, M.A.; Clancy, R.T.; Edgett, K.S.; Edwards, L.J.; Fahle, J.; et al. Mars Reconnaissance Orbiter Mars Color Imager (MARCI): Instrument description, calibration, and performance. *J. Geophys. Res.-Planet* **2009**, *114*, E08S92. [CrossRef]
32. Malin, M.C.; Ravine, M.A.; Caplinger, M.A.; Ghaemi, F.T.; Schaffner, J.A.; Maki, J.N.; Bell III, J.F.; Cameron, J.F.; Dietrich, W.E.; Edgett, K.S.; et al. The Mars Science Laboratory (MSL) Mast cameras and Descent imager: Investigation and instrument descriptions. *Earth Space Sci.* **2017**, *4*, 506–539. [CrossRef] [PubMed]
33. Murchie; Barnouin-Jha, O.; Barnouin-Jha, K.; Bishop, J.; Johnson, J.; McSween, H.; Morris, R. New Insights into the Geology of the Mars Pathfinder Landing Site from Spectral and Morphologic Analysis of the 12-Color Superpan Panorama. 6th International Conference on Mars, Abstract 3060. Available online: https://www.lpi.usra.edu/meetings/sixthmars2003/pdf/3060.pdf (accessed on 18 November 2024).
34. Sánchez-Marañón, M.; Cuadros, J.; Michalski, J.R.; Melgosa, M.; Dekov, V. Identification of iron in Earth analogues of Martian phyllosilicates using visible reflectance spectroscopy: Spectral derivatives and color parameters. *Appl. Clay Sci.* **2018**, *165*, 264–276. [CrossRef]